Proceedings of IMECE2004
2004 ASME International Mechanical Engineering Congress
November 13-19, 2004, Anaheim, California, USA

IMECE2004-62367

EXPERIMENTAL STUDY OF A GAS-LIQUID CYLINDRICAL CYCLONE SEPARATOR PERFORMANCE

Antonio J. Meléndez-Ramírez
Departamento de Termodinámica
Universidad Simón Bolívar

Miguel A. Reyes-Gutiérrez
Departamento de Termodinámica
Universidad Simón Bolívar

Luis R. Rojas-Solórzano
Departamento de Conversión de Energía
Universidad Simón Bolívar

Juan C. Marín-Moreno
CEMFA
Universidad Simón Bolívar

José Colmenares
Gerencia de Exploración y Producción
PDVSA-INTEVEP

ABSTRACT

New data of the experimental performance of a Gas-Liquid Cylindrical Cyclone (GLCC) separator are presented. The data were collected using a 2 3/4" (0.07m) ID GLCC model working with an air-glycerin mixture. The inlet liquid flow rate, the inlet gas flow rate, the tangential liquid velocity inside the separator body and the gas carry under were measured for an operation regime without liquid carry over. The influence of the first three parameters over the gas carry under was established. Results show the separator efficiency is mainly affected by the inlet gas flow rate for the explored conditions with slug flow at the GLCC entrance.

INTRODUCTION

During the last two decades, large efforts have been dedicated to research aiming to the development of multiphase flow compact separators. Today, compact separators are widely used in the industry and particularly in the oil production process, where expensive, heavy and bulky static separators have been traditionally used. The Gas-Liquid Cylindrical Cyclone (GLCC), patented by the University of Tulsa in 1994, is one of these compact devices, developed to separate gas-liquid streams [1]. The GLCC consists on a tangential pipeline connected to a vertical cylindrical body (figure 1). The incoming multiphase stream runs into the cylindrical body through a 30˚-downward inclined tangential pipeline. The gas-liquid mixture enters to the separator and a first separation stage occurs. If the incoming flow velocity is too low, the gravity dominates the inertia and the mixture falls down promoting the stratification or static-like separation of phases. If the flow enters the GLCC body with a mid-high velocity, then a swirling motion begins promoting an inertia-dominated separation process. The centripetal/centrifugal and buoyancy forces drive the gas toward the body centerline and upward to the top, while impelling the liquid toward the wall and bottom of the cylindrical body (see figure 1). The swirling motion of the mixture at the entrance is enhanced by a nozzle. However, the excessive inflow velocity may decrease the separator performance since it also promotes the turbulent mixing of the phases. Gómez et al.[1] recommend a range of tangential velocity of the liquid at nozzle exit between 3 and 6 m/s (10 & 20 ft/s) to ensure a proper operation of GLCC.

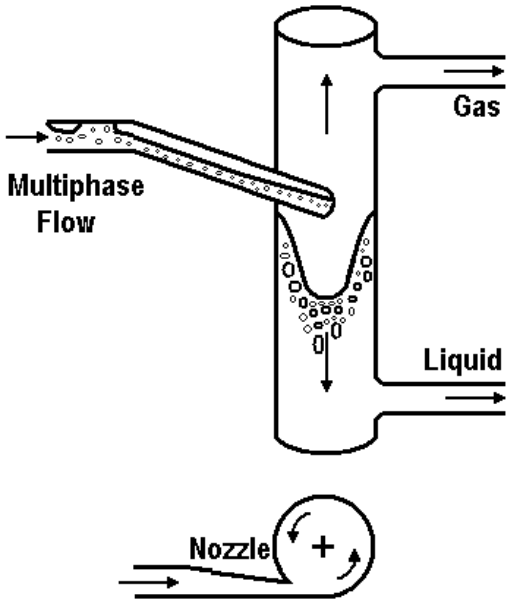

Figure 1: Gas-Liquid Cylindrical Cyclone

The GLCC efficiency is determined by the quality of the outlet streams, i.e., if only gas flows through the top exit and only liquid flows through the bottom exit, then the separator efficiency is 100%. The gas carry under (GCU) and liquid carry over (LCO) are also practical indexes to compute the GLCC efficiency of separation for each exit stream.

During regular operation, inside the GLCC it is established a bubble, slug, churn or annular flow pattern above the injection section, while a vortex sets in underneath. The gas phase accommodates in the vortex core, whereas the liquid phase occupies its periphery [2]. At the present time, it is estimated that there are around 600 GLCC units installed worldwide [1]. Nevertheless, it is not still widely used because of the lack of models that predict accurately its performance.

The most recent research has been focused on developing a mechanistic model capable to reproduce the performance of the GLCC. Arpandi et al [3] proposed the first mechanistic model, which was able to predict the hydrodynamics of the flow inside of the separator. In particular, these authors found a proper estimation of the equilibrium level of liquid, vortex shape, distribution of liquid volume fraction, pressure drop due to the separator and the operation range for non-liquid carry over condition. Motta et al [4] and Erdal et al [5] enhanced the understanding of the hydrodynamics of the single- and multi-phase inside of the GLCC separator through computational fluid dynamics. In addition to the improvements reached by Arpandi et al. [3], a new enhanced mechanistic model, by Gómez et al [6], includes a sub-model to determine the flow pattern and the tangential velocities of the phases at the nozzle exit. Gómez et al. [7] did further improvements to their mechanistic model including expressions for the aspect ratio of each part of the separator, a mathematical sub-model to estimate the behavior of the vortex, and a unified model to establish the particle trajectory. Subsequently, a computational fluid dynamic study was conducted by Matilla et al. [8] to develop a predicting method for the flow field; this tool allowed them to improve the unified model for particle trajectory. Finally, Gómez et al. [9] collected all the contributions to the mechanistic model and implemented them in a computer program, which permits users to design GLCCs and to predict the performance of such devices.

At the present time, there is a limited number of instruments that could allow us to evaluate the performance of the GLCC. This circumstance has prevented the assessment and improvement of current models used to predict the performance of this type of separators. The present study aims to the development of an experimental model on laboratory scale to evaluate the performance of the GLCC. A water-glycerin solution (60% v/v) and air were used as working fluids. The influence of inlet liquid and gas flowrates on gas carry under is reported.

NOMENCLATURE

GLCC=gas liquid cylindrical cyclonic
d = diameter
GVF= gas void fraction, dimensionless
m = mass , kg
ρ = fluid density, kg/m^3
V, v = volume , m^3
μ = fluid viscosity, Pa.s
Q=Inlet flow rate,
R^2=Correlation coefficient
kg/ m^3 = kilograms per cubic meter.
Pa.s = Pascal multiply by second.
B/D = Barrel per day.
Mscf/d = Thousands of standard cubic feet per day.
ft/s = feet per second.
m^3/s = cubic meters per second.
sm^3/s = cubic meters per second at standards conditions.
sft^3/D = cubic feet per day at standards conditions.

SUBSCRIPTS

b = bubble
l = liquid
g = gas
s = sample

S.I. METRIC CONVERSION FACTORS

B x 0.1589873 = m^3
ft x 0.3048 = m
D x 8.64e+004 = s
min x 60 = s

EXPERIMENTAL FACILITIES

The test rig built for the study of the GLCC separator is shown in figure 2.

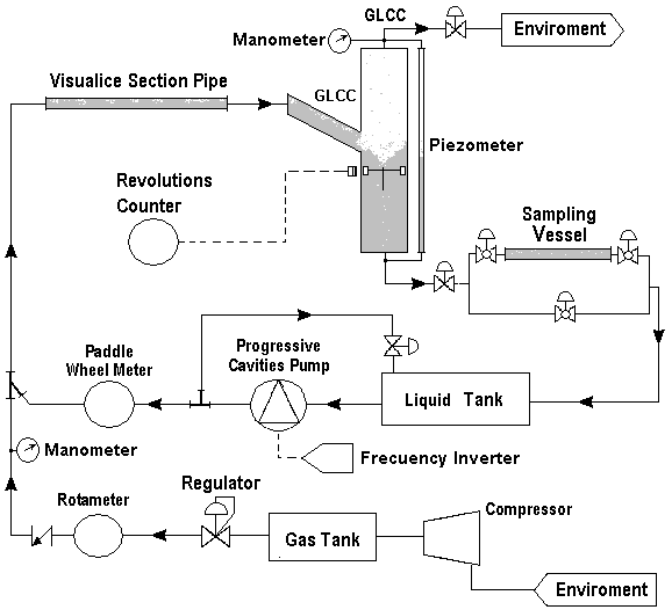

Figure 2: Separator Test Rig

The separator unit was constructed with plexi-glass pipes. This transparent material was chosen to visualize the flow inside of separator. The separator design eases the geometrical configuration changes of the nozzle to study the influence of this parameter on the performance of the separator.

The measured variables throughout the experiments were: the inlet liquid flowrate (Q_l), the inlet gas flowrate (Q_g), the gas void fraction on liquid outlet stream (GVF) and the liquid level inside of separator body. A rotameter was used to measure the inlet gas flowrate. This instrument has an accuracy of $\pm 1.887 \times 10^{-4}$ sm^3/s and a repeatability of $\pm 4.719 \times 10^{-5}$ sm^3/s for a measurement range between 9.439×10^{-4} and 9.439×10^{-3} sm^3/s. The inlet liquid flowrate was quantified by means of a paddlewheel meter, which has an accuracy of $\pm 1.577 \times 10^{-4}$ m^3/s and a repeatability of $\pm 7.885 \times 10^{-5}$ m^3/s for a span fenced

between 4.415×10^{-4} and 7.885×10^{-3} m^3/s. The gas volume fraction at the bottom stream was estimated by taking and weighting samples of it. For such a purpose, a removable vessel was connected to a by-pass line downstream of the bottom exit of the separator (see figure 2). The removable vessel was calibrated to have a volume of $(9.362 \pm 0.007) \times 10^{-4}$ m^3. The mass of every sample was obtained using a semi-analytical balance with an accuracy of 0.0001 kg for a measurement range between 0 and 13 kg.

In previous works, the gas void fraction has been measured at the liquid exit by connecting a modified static separator downstream of that discharge. The alteration consists in coupling a graduated recipient at the gas exit of the static separator, such that in this vessel the gas is collected and its volume is measured while the operation time is registered. With both volume and time, and the outlet liquid flow rate, the gas void fraction at GLCC liquid discharge may be determined. Such metering device has been successful when the working liquid has a low viscosity ($\mu \leq 0.001$ Pa·s). For high viscosity working fluids, the separation of small gas bubbles ($d_b \leq 0.001$ m) at the static separator is incomplete and part of the GLCC gas carry under is not measured. For this reason, this metering device was not adopted in this investigation.

The liquid level inside the separator body was monitored using a piezometer connected between top and bottom of the separator. In order to estimate the magnitude of the centrifugal force exerted over the fluids at the GLCC body, a freely-rotating vane was located 0.90 m above of the separator bottom. Two Bourdon manometers were used to record the pressure at the top of the separator and at the point of liquid-gas mixing on the test rig. Both manometers have an accuracy of 1 psig, while their spans are 0-30 psig and 0-100 psig, respectively.

METHODOLOGY

The experiments were performed as follows:

- The inlet gas and liquid flowrates were established through the rotameter regulation valve and the frequency inverter, respectively.
- Next, the liquid level inside the separator body was adjusted by means of the control valves located at the separator exits. For the range of operating conditions studied, there was no liquid carry over and the gas carry under was minimized as the liquid level of 1.08 m above the GLCC bottom was maintained.
- The inferior outlet stream sample was taken once the system reached the steady state.
- While the experiments were on, the values of the inlet flowrates and the swirling velocity of the vane were registered.
- Every set of experiments ended once the samples were weighted and the gas void fractions at the bottom outlet stream were estimated.
- In order to check the repeatability of the results, the experiment was repeated 5 times for each studied operation condition.

The mass of a sample was related to its gas void fraction through the following equation:

$$m_s = V_v \cdot \left(\rho_g \cdot GVF + \rho_l \cdot (1 - GVF)\right) \quad (1)$$

From this equation, the mass sample, without gas, was calculated assuming that the gas void fraction is equal to zero (GVF=0):

$$m_l = V_v \cdot \rho_l \quad (2)$$

An expression for the estimation of the gas void fraction was obtained subtracting the equation (1) to the equation (2) and rearranging the result to obtain:

$$GVF = \frac{m_l - m_s}{V_v \cdot (\rho_l - \rho_g)} \quad (3)$$

RESULTS

The study considered two nozzle sizes, and their specifications are shown in figure 3. The cross section reduction was the only difference between the nozzles. The working fluids were a 60% v/v water-glycerin[1] solution and air. The flow rates ranges for the liquid and gas at the separator inlet that were studied are presented in table 1. The results are presented in field units to ease their analysis by readers involved in the oil production process, who are familiarized with this unit system.

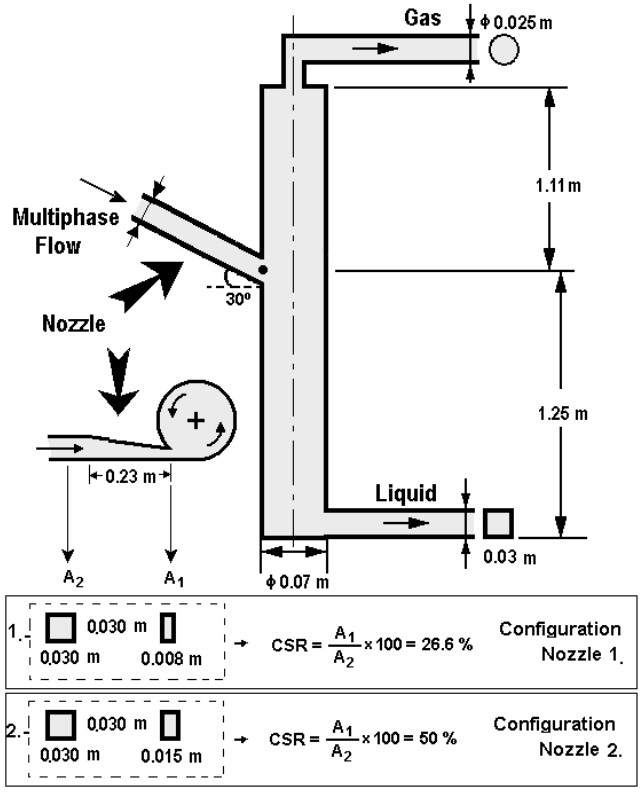

Figure 3: GLCC Model Dimensions

[1] A 60% v/v water-glycerin solution has the following physical properties: $\rho = 1178.68$ kg/m^3 y $\mu = 0.025$ Pa·s

Table 1: Inlet flow rates ranges

Boundary Value	Nozzle 1			
	Q_l (m^3/s)	Q_l (B/D)	Q_g (sm^3/s)	Q_g (sft^3/D)
Minimum	$7.36 \cdot 10^{-4}$	400	$1.61 \cdot 10^{-3}$	$5.00 \cdot 10^{3}$
Maximum	$1.10 \cdot 10^{-3}$	600	$1.16 \cdot 10^{-2}$	$3.62 \cdot 10^{4}$
Boundary Value	**Nozzle 2**			
	Q_l (m^3/s)	Q_l (B/D)	Q_g (sm^3/s)	Q_g (sft^3/D)
Minimum	$5.52 \cdot 10^{-4}$	300	$2.47 \cdot 10^{-3}$	$7.67 \cdot 10^{3}$
Maximum	$1.93 \cdot 10^{-3}$	1050	$1.21 \cdot 10^{-2}$	$3.77 \cdot 10^{4}$

Since the experiments were carried out in absence of liquid carry over, the performance of the separator depends only on gas carry under. For this scenario, the performance of the GLCC might be monitored through either the gas void fraction at the bottom outlet or the gas carry under, since it compares the gas flowrate at the bottom outlet with the gas inlet flow rate. In this study, the gas void fraction was adopted as the measure of the GLCC performance.

NOZZLE 1

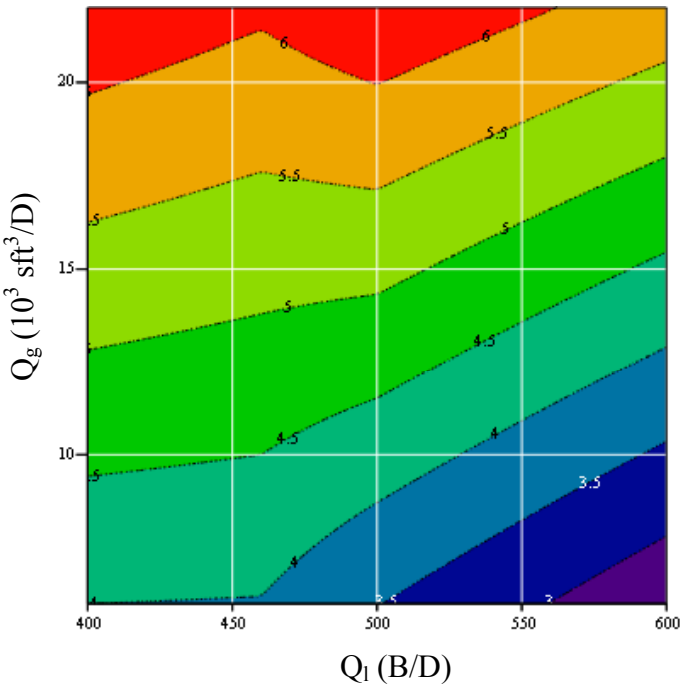

Figure 4: Contour plot of the gas void fraction at the bottom outlet (GVF), as function of the flow rates of inlet liquid (Q_l) and inlet gas (Q_g) for nozzle 1. The plotted values of the gas void fraction at the bottom outlet correspond to the average of the five samples taken in each experiment

The figure 4 shows a contour plot of the gas void fraction at the liquid exit leg as a function of the inlet liquid flow rate and the inlet gas flow rate for nozzle 1. The plotted values of the gas void fraction at the bottom outlet correspond to the average of five samples taken in each experiment. In this figure, it can be noticed that the gas void fraction at the liquid exit is proportional to the inlet gas flow rate for all the operating conditions studied. The relation between the gas void fraction at the liquid discharge and the inlet liquid flow rate is weak. For an inlet gas flow rate smaller than $16 \cdot 10^3$ sft^3/D, the gas void fraction at the bottom exit decreases with the inlet liquid flow rate. On the other hand, when the inlet gas flow rate exceeds $16 \cdot 10^3$ sft^3/D, a clear relationship between the gas void fraction and the inlet liquid flow rate is not observed. A larger number of experiments for gas inlet flow rates bigger than $16 \cdot 10^3$ sft^3/D is required to establish a tendency.

The values of gas void fraction at liquid exit are plotted versus the gas inlet flowrates in the figure 5. A lineal regression of the data is also presented, which was obtained using the least squares method. Additionally, the confidence bands for a probability of 95% are shown. The reported correlation coeficient (R^2) is 0.909, which indicates that the regression is reasonable and that the gas void fraction at bottom outlet is proportional to inlet gas flowrate.

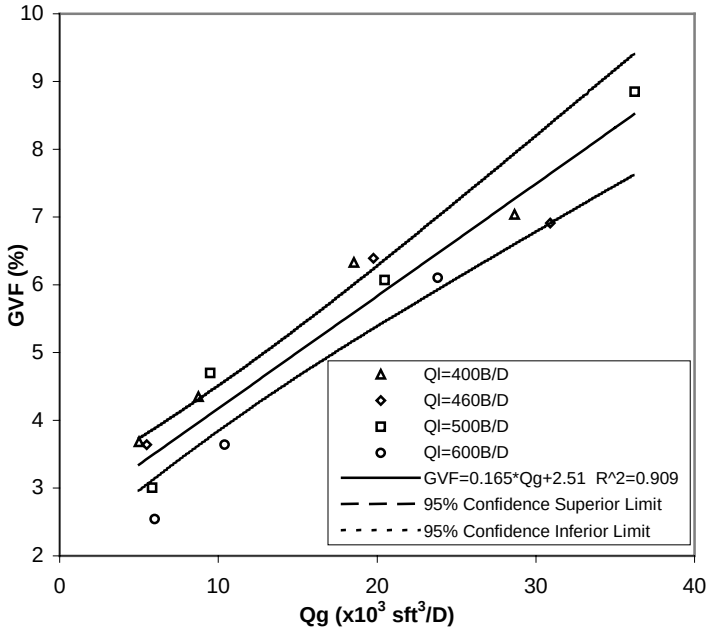

Figure 5: Gas void fraction at bottom outlet (GVF) vs. inlet gas flow-rate (Q_g) for nozzle 1. The plotted values of the gas void fraction at the bottom outlet correspond to the average of the five samples taken in each experiment.

The turbulent mixing of the phases and the breakup of the gas bubbles inside the liquid are collateral effects of the flow acceleration at the nozzle. As the buoyancy force is proportional to bubble volume, the contribution of this force to the separation process decreases. On the other hand, the centrifugal force increases with the flow acceleration. Due to these contrasting influences over the two forces that contribute to separation process, the flow acceleration that optimizes the separator performance is that maximizing the superposition of both buoyancy and centrifugal forces. In addition, it was noticed that the turbulent mixing at the nozzle is strongly dependent of the gas velocity. For this reason, the gas void fraction at the liquid exit is proportional to inlet gas flow rate, as it is evidenced in figures 4 and 5. This fact also explains the

behavior of the gas void fraction at the bottom outlet as a function of the liquid inlet flow rate: for inlet gas and liquid flow rates smaller than $16 \cdot 10^3$ sft^3/D, respectively, the turbulent mixing at the nozzle is low and the separation process is dominated by the centrifugal force. As result, the gas void fraction at the liquid discharge decreases with the liquid inlet flow rate. Finally, for gas inlet flow rates greater than $16 \cdot 10^3$ sft^3/D, the effects of the turbulent mixing at the nozzle and the centrifugal force are comparable and the liquid inlet flow rate seems to have no clear influence over the gas void fraction at the liquid exit.

NOZZLE 2

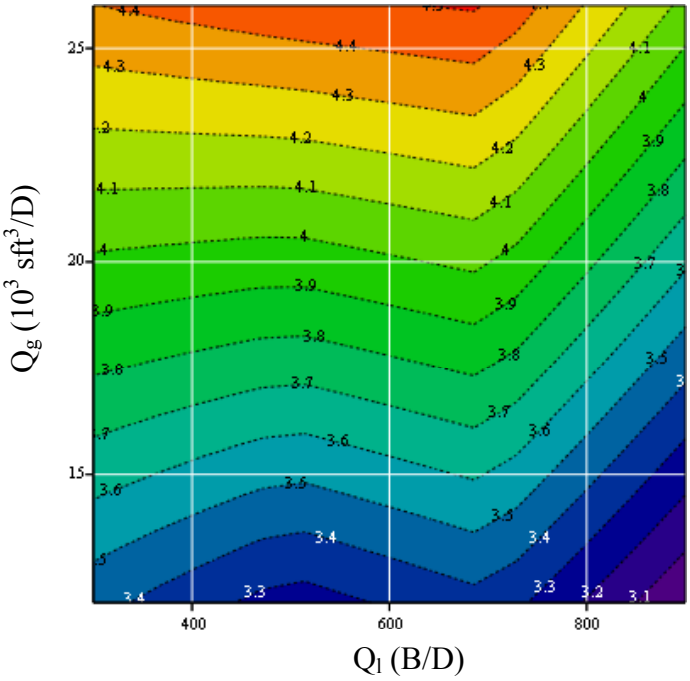

Figure 6: Contour plot of the gas void fraction at the bottom outlet (GVF), as function of the flow rates of inlet liquid (Q_l) and inlet gas (Q_g) for nozzle 2. The plotted values of the gas void fraction at the bottom outlet correspond to the average of the five samples taken in each experiment

A contour plot of the gas void fraction at the bottom outlet as a function of the liquid and gas inlet flow rates is shown in figure 6 for the second nozzle configuration. The values of gas void fraction represented in this plot correspond to an average of the repetitions of each experiment. As in figure 4, it can be observed that the effect of the gas inlet flow rate on the gas void fraction at the liquid exit is more important than the effect of the inlet liquid flow rate. Over the entire range of operating conditions, it can be noticed that the gas void fraction at the bottom outlet increases with gas inlet flow rate. On the other hand, only a weak relationship between the gas void fraction and the liquid inlet flow rate is observed, when it is smaller than 700 B/D. For larger rates, the gas void fraction clearly decreases with the liquid inlet flow rate..

A chart of gas void fraction at the liquid exit versus inlet gas flow rate is presented in figure 7. The data was adjusted to a straight line using the method of least squares, obtaining a correlation coefficient (R^2) of 0.930. In addition, a large number of the plotted points are within the confidence bands. These reasons suggest that the gas void fraction at the bottom discharge is proportional to the inlet gas flow rate for the range of operating conditions studied.

For the nozzle 2, the turbulence mixing of the phases and the breakup of the gas bubbles inside the liquid occurring at the separator nozzle, are relatively low. In consequence, the buoyancy and centrifugal forces have the same order of magnitude and an improvement of the separator performance due to the increase of the centrifugation may be observed. Nevertheless, the magnitude of the gas void fraction at the liquid discharge seems to be determined by the gas inlet flow rate.

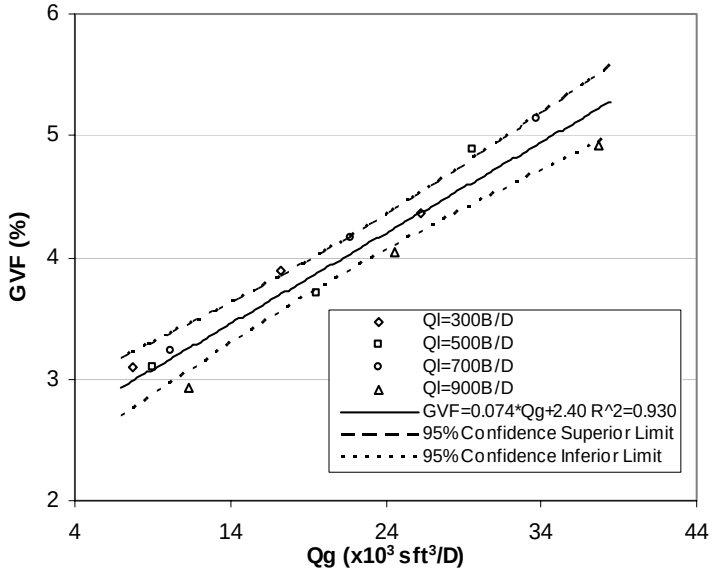

Figure 7: Gas void fraction at bottom outlet (GVF) vs. inlet gas flow-rate (Q_g) for nozzle 2. The plotted values of the gas void fraction at the bottom outlet correspond to the average of the five samples taken in each experiment.

COMPARISON OF THE NOZZLES

If figures 4 and 6 are compared, two important facts can be noticed. First, the magnitude of the gas void fraction at the bottom outlet is bigger for the nozzle 1 than for the nozzle 2; second, the range of operating conditions for which the gas void fraction at the liquid exit decreases with the liquid inlet flow rate, is wider for nozzle 2 than for nozzle 1. As turbulent mixing and bubble breakup have a strong dependence on the velocity of the gaseous phase, the intensities of these phenomena are lesser for the same inlet flow rates since the cross section of nozzle 2 is higher than the transversal area of nozzle 1. Moreover, a reduction on turbulence mixing and bubble breakup permits an increment of the buoyancy force acting on the gas bubble at the vortex, overcoming the deficit of centrifugal force. In consequence, the performance of the separator with nozzle 2 is better than with nozzle 1. Nevertheless, the results presented are not sufficient to rigorously establish a dependence of separator performance with nozzle size. It is necessary to test more nozzle configurations to know this dependence and thus optimize the nozzle design.

Gómez et al. [1] recommend, as a design criterion for the nozzle, that the tangential velocity of the liquid at the entrance of the separator body should be between 10 ft/s (3 m/s) and 20 ft/s (6 m/s). This condition prevents the erosion of the pipes due to excessive velocities, and contributes to ensure a good separator performance. The liquid tangential velocities at the entrance of the separator body for each nozzle studied are presented in table 2. Although the results of this study show that the gas void fraction at the bottom outlet is mainly dependent on the inlet gas flow rate, the second nozzle permits a better separator performance and satisfies the design criterion of Gómez [1] for a bigger number of conditions of operation. When the liquid velocity at the nozzle exit is established, the gas velocity is indirectly fixed; for this reason, such criterion is applicable also for operation regimes in which the separation phenomena are dominated by the gas velocity.

Table 2[2]: Tangential Velocity of the liquid (V_{tl}) at the nozzle exit

Q_l (m^3/s)	Q_l (B/D)	Noz. 1 V_{tl} (m/s)	Noz. 1 V_{tl} (ft/s)	Noz. 2 V_{tl} (m/s)	Noz.2 V_{tl} (ft/s)
$5.5x10^{-4}$	300	4.60	15.09	2.45	8.05
$7.4x10^{-4}$	400	6.13	20.13	3.27	10.73
$9.2x10^{-4}$	500	7.67	25.16	4.09	13.42
$10.4x10^{-4}$	600	9.20	30.19	4.91	16.10
$12.9x10^{-4}$	700	10.73	35.22	5.73	18.78
$14.7x10^{-4}$	800	12.27	40.25	6.54	21.47
$16.6x10^{-4}$	900	13.80	45.28	7.36	24.15
$18.4x10^{-4}$	1000	15.34	50.31	8.18	26.83
$19.3x10^{-4}$	1050	16.10	52.83	8.59	28.18

CONCLUDING REMARKS

The performance of a GLCC separator is studied under different operating conditions. The performance is quantified by accounting for the gas void fraction at the bottom outlet.

For the explored operating conditions, it was found that the gas void fraction at the bottom outlet depends mainly on the inlet gas flow rate. Furthermore, this gas volume fraction is proportional to the inlet gas flowrate. It was noticed that the velocity of the gaseous phase has an important influence on the turbulent mixing and bubble breakup that occur at the nozzle.

The phenomena of turbulent mixing and bubble breakup, happening at the nozzle as a collateral effect to flow acceleration, reduce the size of the bubbles entering into the separator body and therefore, decreases the separation induced by buoyancy. Since the separation process inside the GLCC results from the superposition of the gravitational and centrifugal forces, the net effect of the flow acceleration at the nozzle might be either favorable or adverse for the separator performance. It is important to mention that turbulent mixing and bubble breakup have a strong dependence on physical properties of the phases, mainly on the liquid viscosity and surface tension.

The centrifugal force, strongly related to the liquid inlet flow rate, affects the gas void fraction at the liquid exit only when its contribution to separation is comparable to buoyancy. When this occurs, our experiments show that the gas void fraction at the liquid exit decreases with the liquid inlet flow rate, but this behavior is not monotonic. For low liquid inlet flow rate, the gas void fraction at the liquid outlet seems to be not dependent on the liquid inflow. This behavior is consistent with the physics of the flow inside the separator.

The results of this study show that the GLCC performance is highly conditioned by the nozzle configuration, when the separator handles a viscous liquid ($\mu \geq 0.02$ Pa·s). Moreover, this work evidences the necessity of a major understanding of the flow at the nozzle. Finally, it is recommendable that oncoming research focuses on nozzle design related to the gas void fraction at the liquid exit using, for example, the mixture velocity at the nozzle exit as an independent parameter to characterize this important piece of the GLCC.

[2] These values have been calculated according to reference [1].

ACKNOWLEDGMENTS

The authors would like to thank FONACIT-Venezuela for the financial support to this project. Antonio Melendez-Ramirez wishes to thanks Decanato de Investigación y Desarrollo (DID) at the Universidad Simón Bolívar for supporting his M. Sc. studies.

REFERENCES

[1] Gomez, L., 2003, "Compact Separation Technology", *TUSTP course.* pp. 44-48.

[2] Shoham, O., Kouba, G., 1998, "The state of the art of Gas-Liquid Cylindrical Cyclone Separator," *Journal of Petroleum Technology*, Vol. 50, No. 7, July 1998, pp. 58-65.

[3] Arpandi, I., Joshi, A., Shoham, O., Shirazi, S., Kouba, G., 1996, "Hydrodynamics of Two-Phase Flow in Gas-Liquid Cylindrical Cyclone Separator," SPE 30683, *SPE 70th Annual Meeting*, SPEJ, December 1996, pp. 427-436.

[4] Motta, B., Erdal, F., Shirazi, S., Shoham, O., Rhyne, L., 1997, "Simulation of Single-Phase and Two-Phase Flow in Gas-Liquid Cylindrical Cyclone Separators," FEDSM97-3554, *1997 ASME Fluid Engineering Division Summer Meeting*, June 1997.

[5] Erdal, F., Shirazi, S., Shoham, O., Kouba, G, 1997, "CFD Simulation of Single-Phase and Two-Phase Flow in Gas-Liquid Cylindrical Cyclone Separators," SPE 36645, *SPE 71st Annual Meeting*, SPEJ, Vol. 2, December 1997, pp 436-446.

[6] Gomez, L., Mohan, R., Shoham, O., Kouba, G, 1998, "Enhanced Mechanistic Model and Field Application Design of Gas-Liquid Cylindrical Cyclone Separator" SPE 49174, *SPE 73rd Annual Meeting*, SPEJ, Vol. 5, No. 2, June 2000, pp 190-198.

[7] Gomez, L., Mohan, R., Shoham, O., Kouba, G, 1998, "Aspect Radio Modelling and Design Procedure for GLCC Compact Separator", *20th Annual Energy-Sources Technology Conference and Exhibition*, JERT, Vol. 121, March 1999, pp 49-55.

[8] Mantilla, I., Shirazi, S., Shoham, O., 1999, Flow Field Prediction and Bubble Trajectory Model in Gas-Liquid Cylindrical Cyclone (GLCC) Separators", *ASME Energy Sources Technology Conference and Exhibition*, JERT, Vol. 121, March 1999, pp 9-14.

[9] Gomez, L., Mohan, R., Shoham, O., Marrelli, J., Kouba, G, 1999, "State-of-the-Art Simulator for Field Application of Gas-Liquid Cylindrical Cyclone Separator" SPE 56581, *1999 SPE Annual Technical Conference and Exhibition*, Octubre 1999.